New nitrophenyl-substituted polyperoxotungstate catalyst: A more active and selective for the oxidation of sulfides by hydrogen peroxide

Ahmad M. Al-Ajlouni*, Tariq M. Daiafla, Mohammad El-Khateeb

Department of Applied Chemical Sciences, Jordan University of Science and Technology, Irbid 22110, Jordan

Abstract

Kinetic studies on the catalytic activity of phenylphosphopolyperoxotungstate complexes $[C_{21}H_{37}N]_2[(PhPO_3)\{WO(O_2)_2\}_2\{WO(O_2)_2H_2O\}]$, (**A**) and $[C_{21}H_{37}N]_2[(p\text{-}NO_2Ph(O)PO_3)\{WO(O_2)_2\}_2\{WO(O_2)_2H_2O\}]$, (**B**) toward oxidation of organic sulfides by hydrogen peroxide were carried out in CH_3OH/H_2O mixed solvents. Compound **B** has been prepared for the first time as a modified form of **A**. The presence of a nitro group in **B** increases the electrophilicity of the catalyst, and leads to a higher activity and selectivity for the oxidation of sulfides to sulfoxides by H_2O_2. The reaction rate is found to be first-order in the [catalyst], the [sulfide] and the $[H_2O_2]$ at low $[H_2O_2]$ (<0.01). At higher $[H_2O_2]$ (>0.06 M), the rate becomes almost zero-order in $[H_2O_2]$. The rate of oxidation increases with the sulfide nucleophilicity. Hammett correlations of the rate constants with σ for different substituted diaryl sulfides give negative reaction constants ($\rho \sim -1.2$). The effects of temperature variation, the ratio of water in the solvent, and the solution acidity on the reaction rate are also investigated. A three-membered-ring transition state has been proposed, in which the sulfide attacks the electrophilic O-atom of the W-peroxo species prior to a complete oxygen transfer, as a key step in the reaction mechanism. A radical mechanism has been ruled out.
© 2007 Elsevier B.V. All rights reserved.

Keywords: Polyperoxotungstate; Hydrogen peroxide; Sulfides; Catalytic oxidation; Kinetics and mechanism

1. Introduction

Due to recent environmental concerns, research on the catalytic activation of hydrogen peroxide toward oxidation processes in aqueous solutions has been receiving more attention [1]. Hydrogen peroxide has many advantages over other traditional oxidants including organic peroxides. The major benefit of using H_2O_2 is its environmental acceptability in which the by-product from oxidation is water which eliminates the need for expensive effluent disposal treatments [1c,2]. In addition, H_2O_2 has high oxygen content (47%), exists in high purity, and has acceptable safety in storage and operation [3,4]. Hydrogen peroxide is a mild oxidizing agent, and often activated by homogeneous [5] or heterogeneous [6–8] catalysts. Polyoxometalates (POMs) can combine the selectivity advantages of homogeneous catalysts with stability advantages of

heterogeneous catalysts. This is due to the exclusive inorganic nature of their coordination sphere [9]. Tungsten–POMs exhibit interesting catalytic properties, and has been proved to be useful catalysts for oxidation of different substrates, such as olefins and sulfides [10–12]. A special attention has been given to phosphorus containing POMs due to their high activities [10,9b]. The well known active anions of these complexes are $\{PO_4[WO(O_2)_2]_4\}^{3-}$ and $\{PO_4[MoO(O_2)_2]_4\}^{3-}$. They are usually prepared from the reaction of polyoxometalates with excess H_2O_2 under mild conditions to form the corresponding polyperoxometalates [13,14]. The tungsten complexes have usually shown a better activity than the Mo analogues toward oxidations by H_2O_2 [9]. Griffith et al. [15] have prepared and characterized a phenylphosphopolyperoxometalates, $[NMe_4]_2[(PhPO_3)\{MO(O_2)_2\}_2-\{MO(O_2)_2(H_2O)\}]$; (M = Mo and W). Both Mo and W compounds are active catalysts toward oxidation reactions with H_2O_2 and, as expected, the tungsten complex is more active [11]. The presence of a phenyl group in these systems increases their solubility in organic solvents and promotes their use under homogeneous conditions. In addition, one can utilize the phenyl (or other organic groups) to modify the catalyst in order to enhance the catalyst activity and/or selectivity.

* Corresponding author. Current address: Technische Universität München, Institute Fur Anorganische Chemie, Lichtenbergstr. 4, 85747 Garching, München, Germany. Tel.: +962 2 7201000;
fax: +962 2 7201071/+49 89 289 134743.
 E-mail address: aajlouni@just.edu.jo (A.M. Al-Ajlouni).

Research in the field of the catalytic oxidation of sulfides is promoted due to several reasons. Of these: (a) the synthesis of different chemically and biologically important molecules [16–18] and (b) the removal of sulfur from fuels, and industrial products and wastes, in order to comply with environmental legislations [19]. In addition to hydrodesulfurization (HDS), new methods were recently proposed for the removal of sulfur by oxidation [20,21]. Research on oxidative desulfurization (ODS) has been growing and appeared to be promising. Catalytic oxidation of sulfur-containing compounds by H_2O_2 has been carried out using different homogeneous and heterogeneous catalysts [22–27]. A special attention has been given to catalytic processes in which sulfides are selectively oxidized to sulfoxide [28].

Most POMs activate H_2O_2 by the formation of η^2 or η^1-peroxo moieties from which a nucleophilic reductant abstracts an O-atom [9,11,15]. To enhance the oxygen transfer from the polyperoxometalate to the reductant, the electropositivity of the M-peroxo group should be increased. In this work, we modify the phenylphosphopolyperoxotungstate complex by introducing a nitro group onto the phenyl ring in an attempt to increase the catalyst reactivity toward oxidation of nucleophilic reductants, such as sulfides. The catalytic activities of the new catalyst and the original one (without a nitro group) were investigated, and detail kinetic studies on the oxidation of organic sulfides were carried out under homogeneous conditions in mixed organic-aqueous media.

2. Experimental

2.1. Materials and methods

Diethyl ether, methanol and acetonitrile (HPLC grade, Aldrich) were used without further drying or purification. Water was purified by a Milipore-Q deionization system. H_2O_2 (35%, 3%) was purchased from Scharlau and used as received. Hydrated tungsten trioxide [$WO_3·H_2O$], sodium tungstate dihydrate [$Na_2WO_4·2H_2O$], organic sulfides and methylphenyl-sulfoxide, phenylphosphonic acid [$C_6H_5P(O)(OH)_2$], (4-nitrophenyl)-phosphoryldichloride [$4-O_2NC_6H_4OP(O)(Cl)_2$], and cetylpyridinium chloride [$C_{21}H_{37}NCl$] were used as purchased from Aldrich. Stock solutions of hydrogen peroxide were prepared in deionized water by diluting commercial samples of H_2O_2 (3% or 35%). The diluted stock solutions were standardized daily by iodometric method [29].

FT-IR measurements were carried out using a Nicolet-Impact 410 FT-IR spectrometer (solid KBr disk). The NMR spectra were obtained on a Bruker DXP-400 spectrometer (^{31}P, 162 MHz, using external H_3PO_4 as reference; ^{1}H, 400 MHz, TMS) in CD_3CN solutions. The UV–vis spectra were recorded using Shamadzu UV-2401-PC spectrometer.

2.2. Synthesis of the catalysts

[$C_{21}H_{37}N$]$_2$[(PhPO$_3$){WO(O$_2$)$_2$}$_2${WO(O$_2$)$_2$H$_2$O}] (**A**) was prepared as previously described [15], with cetylpyridinum chloride instead of NMe$_4$Cl. When 2.5 g (10 mmol) of

WO$_3$·H$_2$O was used, the yield was 3.3 g (2.1 mmol, 63%). The product was identified by UV–vis, IR and NMR spectroscopic methods. IR (KBr, cm^{-1}): 958vs, 956vs $\nu_{(M=O)}$, 767s, 768s $\nu_{(MO_2)}$, 851vs, 847vs $\nu_{(O-O)}$. ^{1}H NMR (CD$_3$CN) δ (ppm): the phenyl protons appear at 7.3 (m, 5H). ^{31}P (NMR): 15.77 ppm.

[$C_{21}H_{37}N$]$_2$[(p-NO$_2$Ph(O)-PO$_3$){WO(O$_2$)$_2$}$_2${WO(O$_2$)$_2$H$_2$O}] (**B**) was prepared by slight modification of the method used to prepare compound **A** above.

A suspension of hydrated tungsten trioxide, WO$_3$·H$_2$O (2.5 g, 10 mmol) in 30% H$_2$O$_2$ (8 mL) was stirred for 7–8 h at 45–50 °C. This solution was filtered to remove undissolved residue, then (4-nitrophenyl)-phosphoryldichloride (0.8 g, 3.5 mmol) in water (10 mL) was added followed by dropwise addition of cetylpyridinium chloride, C$_{21}$H$_{37}$NCl, (2.4 g, 7.0 mmol). The mixture was stirred in an ice-bath (0 °C) until a precipitate was formed. The solid product was isolated (by filtration), washed successively with cold ethanol (2× 5 mL) and diethyl ether (2× 10 mL), and air dried. Yield 3.2 g (59%). Elemental analysis (C, 34.15% H, 5.12%; N, 2.49% is in agreement with the calculated values for C$_{48}$H$_{80}$N$_3$O$_{22}$PW$_3$ (C, 35.28%; H, 4.90%; N 2.57%). Attempts to obtain suitable crystals for X-ray crystallography were not successful. The pure compound was characterized by IR and NMR spectroscopy. IR (KBr, cm^{-1}): 959vs $\nu_{(M=O)}$, 755s $\nu_{(MO_2)}$, 887vs $\nu_{(O-O)}$, 1468s, 1381s $\nu_{(NO_2)}$. ^{1}H NMR (CD$_3$CN) δ (ppm): the p-nitrophenyl protons appear at 7.5 (m, 2H) and 8.2 (m, 2H). ^{31}P (NMR): 27.35 ppm.

2.3. Kinetic studies

2.3.1. Oxidation of sulfides

The reactions were carried out in mixed CH$_3$OH/H$_2$O solvents. Kinetic data were collected by following the absorbance change due to the loss of the sulfide and the formation of the product(s) in the region 260–300 nm, using UV–vis spectrometer (Shimadzu UV-2401-PC). At these wavelengths, the absorbance of the catalyst is minimal at the concentrations employed. Quartz cuvettes with optical path of 1.0 cm (V_T = 3.0 mL) were used. The temperature was kept constant at 25.0 ± 0.5 °C throughout the entire series of experiments. The solution ionic strength was not maintained for these reactions. When the effect of solution acidity was studied, the solution pH was regulated by HClO$_4$ and was checked with a pH-meter. Initial rate and pseudo-first-order conditions applied in different protocols.

2.3.1.1. Initial rate method.
In this method, the full kinetic trace of the reaction was not always acquired. Reaction mixtures were prepared in a spectrophotometric cell with the last reagent added being the sulfide. The initial rates were calculated from the first 5% of the curves by using the following equation:

$$\text{i.r.} = -\left(\frac{1}{b\Delta\varepsilon_\lambda}\right) \times \frac{\Delta\text{Abs}_i}{\Delta t} \tag{1}$$

where b is the optical path length, $\Delta\varepsilon_\lambda$ is the total change in the molar absorptivity at λ, and ΔAbs_i is the initial change in the absorbance.

2.3.1.2. Pseudo-first-order method. Except when the effect of [H_2O_2] was studied, all UV–vis experiments were done in the presence of large excess [H_2O_2] (=0.1 M) over the sulfides and the catalysts. The sulfides concentrations were (0.05–0.50 mM) while the catalysts concentrations were (0.005–0.05 mM). The change in the absorbance of sulfides with time followed first-order kinetics. The observed-first-order rate constants were evaluated by nonlinear least-square fitting of the absorbance–time curves to a single exponential equation (Eq. (2)):

$$Abs_t = Abs_\infty + (Abs_o - Abs_\infty)\exp(-k_\psi t) \tag{2}$$

where Abs_t, Abs_o and Abs_∞ are the absorbance at any-time, initial and final absorbance, respectively, and k_ψ is the observed-first-order rate constant. The data were analyzed by KaleidaGraph program, version 3.09.

2.3.2. Oxidation of the sulfoxide

The oxidation of methylphenylsulfoxide by H_2O_2 as catalyzed by **A** and **B** were studied by ^{1}H NMR spectroscopic method in methanol-d4/D_2O (9:1, v/v). The reactions were carried out under pseudo-first-order conditions (as shown above) in the presence of large excess [H_2O_2] (=1.0 M) over the sulfides (0.02 M) and the catalysts. The catalysts concentrations were varied in the range 0.04–0.4 mM. ^{1}H NMR spectra were recorded every 5 min for the first hour, then every 20 min for 3–5 h. The changes in the relative peak intensities with time of the CH_3 protons at 2.73 ppm followed first-order kinetics. The observed-first-order rate constants were evaluated by nonlinear least-square fitting of the intensity–time curves to a single exponential equation, Eq. (2).

3. Results and discussion

3.1. The catalysts

The new phosphopolyperoxotungstate complex ([$C_{21}H_{37}N$]$_2$ [(p-NO_2Ph(O)-PO_3)–{$WO(O_2)_2$}$_2${$WO(O_2)_2H_2O$}]) (**B**) was prepared for the first time using a modified procedure of a literature method [15]. It was characterized by IR, and ^{1}H and ^{31}P NMR spectroscopic techniques and the spectroscopic data were compared with that of compound **A**.

We were unable to get suitable crystals of **B** for X-ray crystal structure determination. The compound was always precipitate as fine solid material. However, the similarities between the spectroscopic data of **B** and the spectroscopic data reported for the known complexes; ([R_4N]$_2$[(PhPO$_3$){MO(O$_2$)$_2$}$_2${MO(O$_2$)$_2H_2O$}]), (M = Mo or W) indicate that compound **B** may have a similar structure, Scheme 1.

The X-ray crystal structure of the trinuclear compound, ([R_4N]$_2$[(PhPO$_3$){MO(O$_2$)$_2$}$_2$–{MO(O$_2$)$_2H_2O$}]), shows that two M atoms are identical, each have two peroxo and an oxo groups, and the third M has similar groups in addition to a water molecule as shown above [15].

In this study, we have chosen to investigate the activities of the above tungsten catalysts because they are significantly
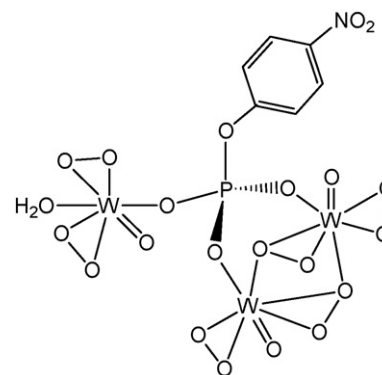
Scheme 1. A proposed structure for compound **B**.

more active than the analogues polyperoxomolybdate [11]. Also, the presence of a phenyl group and a large organic counter-cation (cetylpyridinium) enhance the catalyst solubility in organic solvents in which homogeneous catalytic reactions can be studies. In addition, a nitro group was introduced to increase the electrophilicity of the W-peroxo group in an attempt to increase its activity toward oxygen transfer to a nucleophilic substrate. Aromatic sulfides are soft nucleophiles and good reductants. For kinetic studies, aromatic sulfides, such as thioanisole, can be followed by recording the absorbance change in the UV region (260–300 nm) or by NMR spectroscopic methods.

3.2. Identity of the oxidation products

Sulfide oxidation by H_2O_2 catalyzed by compounds **A** and **B** was monitored via ^{1}H NMR spectroscopy to determine the identity of the products. With thioanisole, CH_3-S-Ph, the CH_3 signal is particularly informative. The CH_3 protons in thioanisole show up as a singlet at 2.55 ppm. In the sulfoxide and the sulfone, the CH_3 protons chemical shifts are at 2.73 and 2.86 ppm, respectively. The NMR measurements were carried out in methanol-d4/D_2O (9:1, v/v) with H_2O_2:cat:sulfide ratio 100:0.2:20 (mM), respectively. ^{1}H NMR spectra were recorded every 5 min for the first hour, then every 20 min for 3 h. The changes in the relative peak intensities with time for thioanisol and its oxidation products are shown in Fig. 1. In the reaction catalyzed by **A**, the sulfoxide signal reaches maximum after ∼50 min with 50% accumulation. The relative amount of sulfone at this time was ∼25%. After 2 h, the sulfide signal at 2.55 ppm disappeared almost completely, and the sulfoxide to sulfone ratio was ∼1:4 (Fig. 1). When the reaction is catalyzed by **B**, under exactly the same conditions, the sulfoxide reaches maximum after ∼20 min with 70% accumulation, and the sulfone signal was less than 15%. After 50 min, the sulfide was completely reacted. These results show that the new catalyst (**B**) is more active toward sulfide oxidation to sulfoxide. This has been confirmed by the detail kinetic studies that carried out on the activation of H_2O_2 by both catalysts, and the formation of sulfoxide and sulfone, as shown below. The kinetic analysis of the data in Fig. 1 is also presented later in this paper.
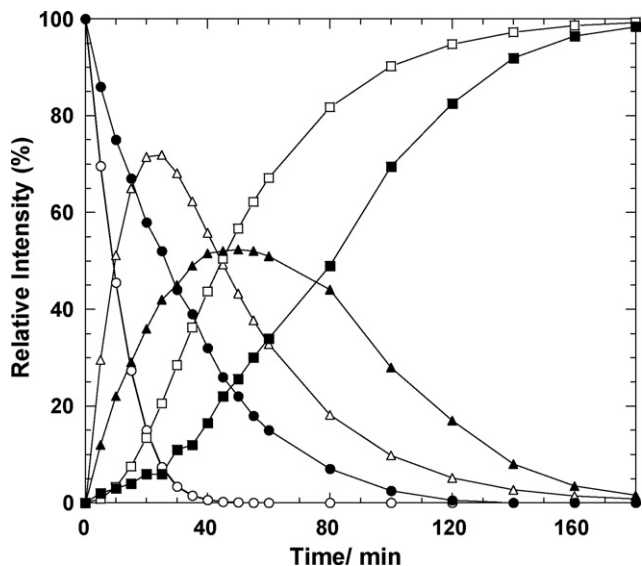
Fig. 1. The changes in the relative peak intensities with time of thioanisol (●, ○ at $\delta = 2.55$ ppm), and its sulfoxide (▲, △ at $\delta = 2.73$ ppm) and sulfone (■, □ at $\delta = 2.86$ ppm) during the oxidation of thioanisol by H_2O_2 catalyzed by **A** (closed legend) and **B** (opened legend) in CD_3OD at 25 °C with $[H_2O_2] = 0.1$ M, [thioanisol] = 0.02 M and [cat] = 0.2 mM.

3.3. Kinetics

The NMR data (Fig. 1) shows the general behavior of reactions that involve oxidation of an organic sulfide; the sulfide disappearance, the build up and decay of the sulfoxide and the sulfone formation (Eq. (3)):

$$\text{(Eq. 3 reaction scheme)}$$

(3)
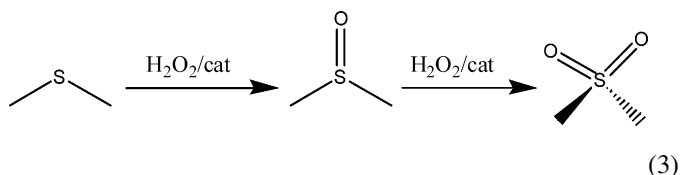
The sulfide usually acts as a nucleophilic reductant, while the sulfoxide is electrophilic [30]. This dual behavior of the sulfur atom in the sulfide and the sulfoxide makes it a suitable system to investigate a nucleophilic versus an electrophilic behavior of an oxidant. On the other hand, one can control the product formation by modifying the oxidant nucleophilicity or electrophilicity. Polyoxoperoxometalates of high valent early transition metals are usually acidic and one expects an electrophilic behavior when reacting with a reductant, i.e. more active toward nucleophilic reductants. Therefore, a nitro group was added in **B** to enhance its electrophilicity.

3.3.1. The catalysts' activities

Kinetic experiments on the activity of each catalyst (**A** and **B**) toward oxidation of thioanisol by H_2O_2 were carried out in CH_3OH/H_2O (9:1, v/v) at 25 °C with $[H_2O_2] = 0.1$ M, [thioanisol] = 0.4 mM and [cat] varied in the range 0.005–0.05 mM. The change in absorbance with time due to the reaction of thioanisol was recorded at 285 nm. Under these conditions, the reaction rates were independent on $[H_2O_2]$ (as will be explained later), and the reaction follow a pseudo-
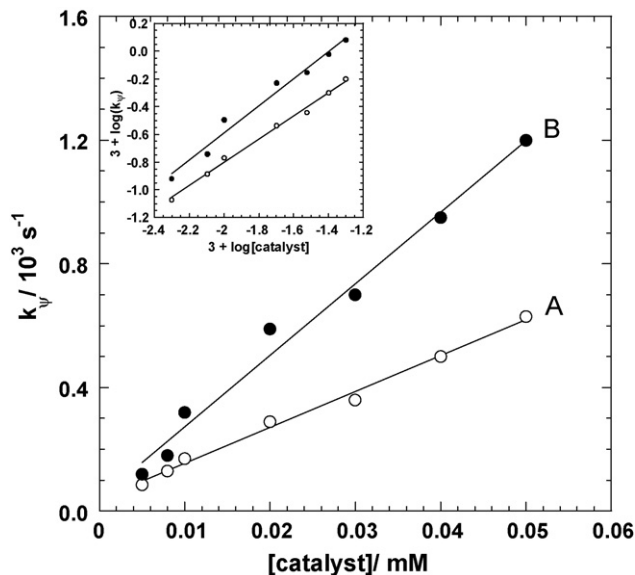

Fig. 2. Variation of the pseudo-first-order rate constants with the catalyst concentrations for the oxidation of 0.2 mM thioanisol with H_2O_2 (0.1 M) as catalyzed by **A** and **B**. The slopes are the catalyzed second-order rate constants and the intercepts are the uncatalyzed rate constants; k_{cat}/k_{uncat} of **A** and **B** are 2.3×10^2 and 5.6×10^2, respectively. The inset shows the log plots.

first-order kinetic. The absorbance–time curves were fit to a first-order exponential decay equation (Eq. (2)). The orders of the reactions with respect to the catalyst concentrations were determined from plots of $\log(k_\psi)$ against $\log[\text{catalyst}]$ and found to be 0.87 ± 0.04 and 0.98 ± 0.07 for **A** and **B**, respectively (Fig. 2 inset). This indicates, within experimental error, that the reaction in both cases is first-order in the [catalyst]. The observed-first-order rate constants (k_ψ) obtained for each catalyst were varied linearly with the catalyst concentration (Fig. 2). The slopes of the lines represent the catalyzed rate constants and the intercepts are the uncatalyzed rate constants. The catalyzed rate constant of **B** is almost twice that of **A** under the same conditions ($k(\mathbf{B}) = 26.4 \pm 1.3$ M^{-1} s^{-1} and $k(\mathbf{A}) = 12.7 \pm 0.4$ M^{-1} s^{-1}). These results show that the presence of a nitro group on **B** increases the reactivity to oxidize thioanisol by H_2O_2. Similar experiments were carried out on the oxidation of other aromatic sulfides. The values of the catalyzed rate constants for reactions catalyzed by both catalysts (**A** and **B**) are listed in Table 1. In all cases, the catalyzed rate constant for **B** is almost twice that of **A** indicating that the oxidation mechanism is probably the same for all sulfides.

Table 1

The catalyzed rate constant for the oxidation of different aromatic sulfides by H_2O_2 catalyzed by **A** or **B**, in CH_3OH/H_2O (9:1, v/v) at 25 °C with $[H_2O_2] = 0.1$ M, [sulfide] = 0.4 mM and [cat] varied (0.005–0.05 mM)

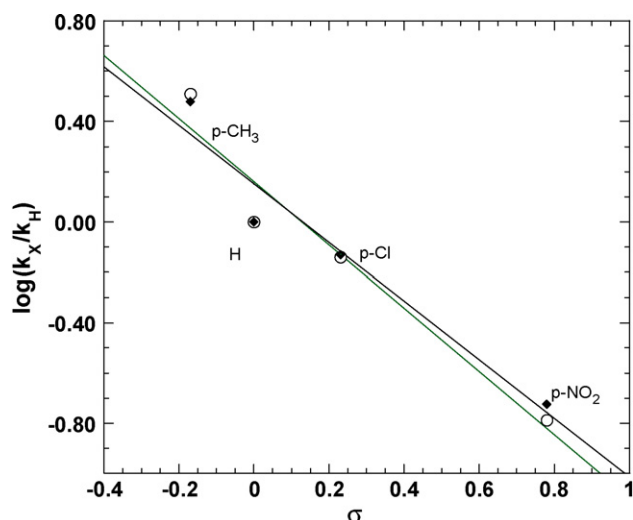| Sulfide	$k(\mathbf{A})$ (M^{-1} s^{-1})	$k(\mathbf{B})$ (M^{-1} s^{-1})
H_3C-S-Ph	12.7 ± 0.4	26.4 ± 1.3
$[(p\text{-}CH_3)C_6H_4]_2S$	0.58 ± 0.05	1.23 ± 0.06
Ph-S-Ph	0.18 ± 0.02	0.38 ± 0.05
$(p\text{-}ClC_6H_4)_2S$	0.13 ± 0.03	0.27 ± 0.04
$(p\text{-}O_2NC_6H_4)_2S$	0.034 ± 0.006	0.062 ± 0.005

Fig. 3. The Hammett correlation of $k(\mathbf{A})$ and $k(\mathbf{B})$ for the oxidation of p-substituted diphenyl sulfides (shown in Table 1) by H_2O_2 as catalyzed by $\mathbf{A}$ (♦) and $\mathbf{B}$ (○) against σ. The reaction constants are $\rho(\mathbf{A}) = -1.16$ and $\rho(\mathbf{B}) = -1.25$.

The data in Table 1 show that the reactivity of the sulfides increases with their nucleophilicity. Indeed, Hammett correlations of the rate constants of p-substituted diphenyl sulfide with σ, $(\log(k_X/k_H)) = \rho\sigma)$, were linear, and give values; $\rho(\mathbf{A}) = -1.16 \pm 0.20$ and $\rho(\mathbf{B}) = -1.25 \pm 0.21$ (Fig. 3). Actually, the ρ values of both catalysts are considered the same within the experimental error associated with each measurement. Similar negative values of ρ have been reported for the oxidation of diaryl sulfides by H_2O_2 catalyzed by metal-peroxo catalysts of Mo(VI), W(VI) and Re(VII) [5a,31] which suggest the buildup of a positive charge at the reaction center. The linear correlation indicates that all the sulfides are oxidized by the same mechanism.

3.3.2. The rate law

It is quite complicated to study the complete kinetic profile of these oxidation reactions due to the fact that two oxidation steps (sulfoxide and sulfone formation) are present in the reaction and presumably other polyoxoperoxotungstate intermediates are generated from the catalyst reduction. Therefore, initial rate method (see Section 2) was used to determine the rate law, in which the data obtained from the beginning of the reaction ($\Delta abs_i \leq 5\%$) were used for kinetic analysis. This would minimize the involvement of more than one form of the catalyst, and be limited to the sulfide oxidation.

Studies on the catalytic activity of $\mathbf{A}$ (or similar POMs) toward oxidation of different substrates, including sulfides, by H_2O_2 have shown that the polyperoxotungstate with the maximum number of peroxo groups is the active form of the catalyst. This species is the dominant species (or the only one exists) in the presence of large excess H_2O_2 [10,11]. Upon oxidation of the sulfide, it loses one oxygen atom from one of the peroxo groups to form an intermediate with one less peroxo group. Then, the active peroxo species is regenerated from the reaction of this intermediate with H_2O_2. A proposed reaction sequence that may be involved in this oxidation is shown in Scheme 2. The
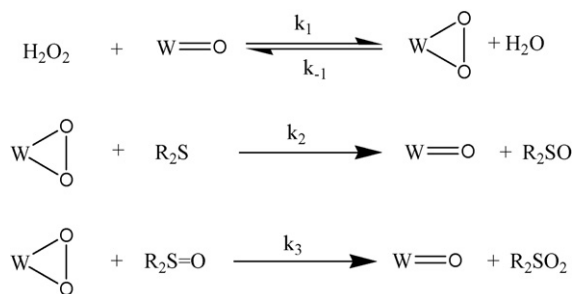
Scheme 2.

first step must be reversible to regenerate the catalyst, followed by two oxidation steps which lead to sulfoxide and sulfone.

The kinetic data were collected by following the absorbance changes due to the decrease in the sulfide concentration with time, so the rate can be expressed as follows:

$$\text{rate}(v) = -\frac{d[R_2S]}{dt} = k_2[WO_2][R_2S] \tag{4}$$

If $k_2[R_2S] + k_{-1} \gg k_1[H_2O_2]$, a steady-state approximation on WO_2 (the peroxo species) can be applied. With the mass balanced equation $[W]_T = WO_2 + WO$, the rate of the reaction can be expressed as follows:

$$v = -\frac{d[R_2S]}{dt} = \frac{k_1k_2[W]_T[H_2O_2][R_2S]}{k_{-1} + k_1[H_2O_2] + k_2[R_2S] + k_3[R_2SO]} \tag{5}$$

Under initial rate conditions, the involvement of the second oxidation would be negligible, and the initial rate can be simplified as shown below:

$$v_i = -\frac{\Delta[R_2S]_i}{\Delta t} = \frac{k_1k_2[W]_T[H_2O_2]_i[R_2S]}{k_{-1} + k_1[H_2O_2]_i + k_2[R_2S]_i} \tag{5a}$$

On the other hand, if $k_1[H_2O_2] + k_{-1} \gg k_2[R_2S]$, then an equilibrium (in the first step, $K_1 = k_1/k_{-1}$) is established before the active species reacts with the sulfide or the sulfoxide. In this case, both oxidation rates are first-order in $[WO_2]$ which depends on the total concentration of the catalyst ($[W]_T$), $[H_2O_2]$, and the value of K_1. The rate laws for sulfide and sulfoxide oxidation can be expressed as follows:

$$v = -\frac{d[R_2S]}{dt} = \frac{K_1k_2[W]_T[H_2O_2][R_2S]}{1 + K_1[H_2O_2]} \tag{6a}$$

$$v' = -\frac{d[R_2SO]}{dt} = \frac{K_1k_3[W]_T[H_2O_2][R_2SO]}{1 + K_1[H_2O_2]} \tag{6b}$$

3.3.3. Variation of the sulfide concentration

Kinetic experiments on the oxidation of thioanisol were carried out at constant $[H_2O_2] = 0.1$ M and [catalyst] = 0.05 mM, and [thioanisol] was varied in the range 0.05–0.5 mM. An equilibirium between the catalyst and H_2O_2 was established before thioanisol was added. With high ratio of H_2O_2:catalyst (~2000:1), we assumed that the catalyst exists in the final peroxo form (Scheme 1). The change in the absorbance at 285 nm due to the loss of thioanisol was recorded with time. The initial rates were calculated from the first 2–5% of the absorbance–time curves using Eq. (1). The change in the molar absorptivity ($\Delta\varepsilon$)
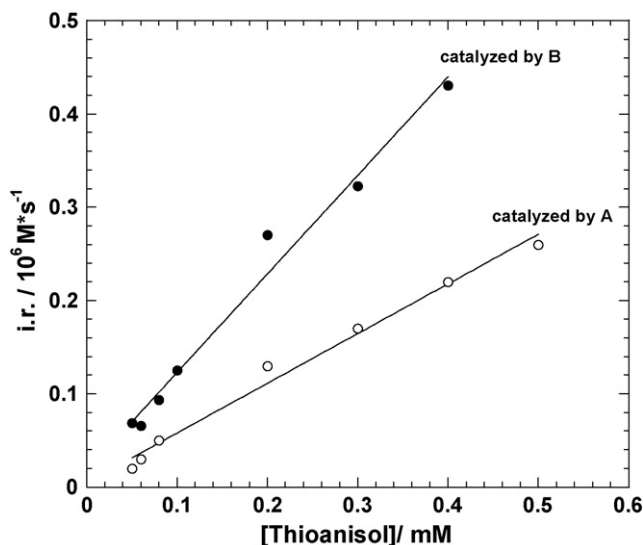
Fig. 4. The initial rate of oxidation of thioanisol by [H$_2$O$_2$] (0.1 M) catalyzed by [**A**] (0.05 mM) and [**B**] (0.05 mM) varies linearly with [thioanisol] in CH$_3$OH/H$_2$O (9:1, v/v) at 25 °C. The fit to Eq. (7) gave $k_3 = 10.6 \pm 0.5$ and $21.1 \pm 1.3\,\mathrm{M^{-1}\,s^{-1}}$ for the reactions catalyzed by **A** and **B**, respectively.

was estimated from the total absorbance change during the whole reaction. Under these conditions, the initial rates of oxidation of thioanisol by H$_2$O$_2$ catalyzed by both catalysts were varied linearly with [thioanisol] (Fig. 4). The orders of the reactions with respect to [thioanisol] were determined from plots of log(i.r.) against log[thioanisol] as 1.07 ± 0.03 and 0.94 ± 0.01 for the reactions catalyzed by **A** and **B**, respectively. These results show that the reaction in both cases is first-order in the sulfide concentration. It also indicates that $k_1[\mathrm{H_2O_2}] + k_{-1} \gg k_2[\mathrm{R_2S}]$, so Eq. (6a) is valid under these conditions. In the presence of high [H$_2$O$_2$], $K_1[\mathrm{H_2O_2}]$ would be significantly greater than 1, and Eq. (6a) can be simplified to

$$v = -\frac{\mathrm{d[R_2S]}}{\mathrm{d}t} = k_2[\mathrm{W}]_{\mathrm{T}}[\mathrm{R_2S}] \tag{7}$$

Based on Eq. (7), the slopes of Fig. 4 equal $k_2[\mathrm{W}]_{\mathrm{T}}$ ([W]$_{\mathrm{T}}$ = the total concentration of the catalyst). The values of k_2 were determined (using [W]$_{\mathrm{T}} = 0.05$ mM) as 10.6 ± 0.5 and $21.1 \pm 1.3\,\mathrm{M^{-1}\,s^{-1}}$ for the reactions catalyzed by **A** and **B**, respectively. These values are in agreement with the rate constant values obtained from studies on the catalyst variation under similar conditions; $k_A = 12.7 \pm 0.4$ and $k_B = 26.4 \pm 1.3\,\mathrm{M^{-1}\,s^{-1}}$ (Table 1).

3.3.4. Variation of H$_2$O$_2$ concentration

Kinetic measurements were carried out with a constant [catalyst] (=0.05 mM) and a constant concentration of thioanisol of 0.4 mM. The concentration of H$_2$O$_2$ was varied in the range 1–100 mM. The initial rates were calculated from the absorbance–time curves as previously described. Variation of the initial rate with [H$_2$O$_2$] for reactions catalyzed by **B** is shown in Fig. 5. At low [H$_2$O$_2$] (≤ 5 mM), the dependence is almost linear (i.e. first-order in [H$_2$O$_2$]). This dependence decreases at higher [H$_2$O$_2$] and becomes independent (zero-order) when [H$_2$O$_2$] reaches about 80 mM. The data in Fig. 5 were fitted to
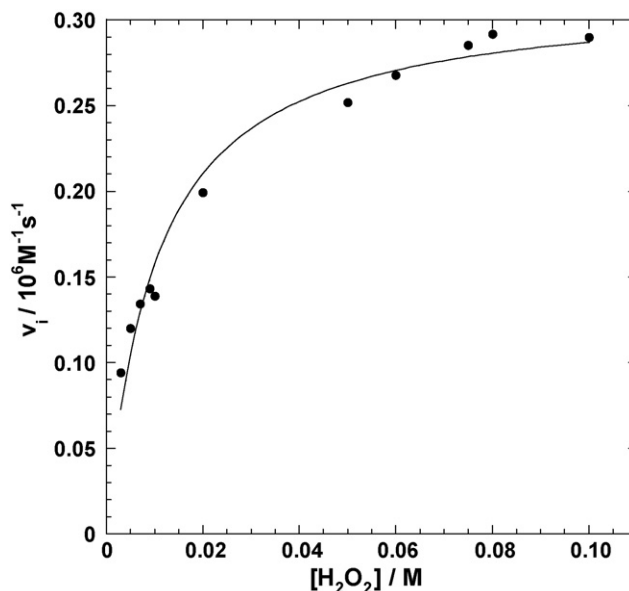

Fig. 5. A plot of the initial rate of oxidation of thioanisol (0.4 mM) by H$_2$O$_2$ catalyzed by the catalyst **B** (0.05 mM) against [H$_2$O$_2$]. The data fits to Eq. (5a).

Eq. (5a) and gave the values of $k_1 \times k_2 = 30.1 \pm 3.5$, and $k_{-1} + k_2$ [R$_2$S] $= 0.015 \pm 0.005$. The rate constant k_1 was calculated using the value of $k_2 = 21.1\,\mathrm{M^{-1}\,s^{-1}}$ to be $k_1 = 1.5 \pm 0.3\,\mathrm{M^{-1}\,s^{-1}}$. The value of k_{-1} cannot be determined accurately. However, it was estimated as $k_{-1} \leq 0.007\,\mathrm{s^{-1}}$ and the equilibrium constant $K_1 \geq 2 \times 10^2$. Similar experiments and kinetic analysis were carried out using the catalyst **A**. The following values were obtained: $k_1 = 0.5 \pm 0.1\,\mathrm{M^{-1}\,s^{-1}}$, $k_{-1} \leq 0.004\,\mathrm{s^{-1}}$ ($K_1 \geq 1 \times 10^2$) and $k_2 = 10.6 \pm 0.5\,\mathrm{M^{-1}\,s^{-1}}$.

3.4. Sulfide versus sulfoxide oxidation

The NMR data in Fig. 1 shows clearly the two-oxidation steps, formation of the sulfoxide from the sulfide followed by oxidation of the sulfoxide to form the sulfone. The change in the NMR signal intensity at 2.55 ppm (sulfide signal) with time was curved but not exponential. It is exhibiting an approach toward linearity at the beginning of the reaction but becoming more nearly exponential during the latter stages (Fig. 1). The last 20% of the intensity–time curves (after 60 and 20 min for the reactions catalyzed by **A** and **B**, respectively) fit very well to a first-order exponential decay equation (Eq. (2)). The observed-first-order rate constants obtained from this fitting were used to calculate the values of the second-order rate constants for the oxidation of thioanisol according to Eq. (7), where $k_\psi = k_2[\mathrm{W}]_{\mathrm{T}}$, assuming the reaction rate is independent on [H$_2$O$_2$], and the [W]$_{\mathrm{T}}$ is constant during the reaction. The values of k_2 determined by this method were similar (within 5–10% error) to that obtained previously from the UV experiments using the initial rate method.

3.5. The rate of oxidation of the sulfoxide generated from the sulfide

The change in the sulfoxide NMR-signal intensity with time consists of two stages (biphasic), as shown in Fig. 1. The val-

Table 2
The rate constants for the oxidation of sulfides (k_2) and oxidation of sulfoxides (k_3) by the active forms of the catalysts **A** and **B** based on Scheme 2, in CH_3OH/H_2O (9:1, v/v) at 25 °C with $[H_2O_2] = 0.1$ M

Sulfide	Catalyst A		Catalyst B	
	k_2 (k_3) (M^{-1} s^{-1})	k_2/k_3	k_2 (k_3) (M^{-1} s^{-1})	k_2/k_3
Methylphenyl sulfide	10.6 ± 0.5 (4.8 ± 0.1)	2.2	21.1 ± 1.3 (3.1 ± 0.2)	6.8
Di-(*p*-toulyl) sulfide	0.58 ± 0.05 (0.28 ± 0.03)	2.1	1.23 ± 0.06 (0.20 ± 0.03)	6.2
Diphenyl sulfide	0.18 ± 0.02 (0.08 ± 0.02)	2.3	0.38 ± 0.05 (0.07 ± 0.03)	5.4

ues of the second-order rate constants for the oxidation of sulfoxide to sulfone (second stage) were determined from the intensity–time curves after the sulfide was completely reacted (after 120 or 50 min for the reaction catalyzed by **A** or **B**, respectively). At this stage of reaction ([sulfide] = 0), assuming that the catalyst concentration remains constant and the reaction rate is independent on the $[H_2O_2]$ ($[H_2O_2] > 0.06$ M, see Fig. 5), the rate equation for the sulfoxide oxidation (Eq. (6b)) becomes

$$v' = -\frac{d[R_2SO]}{dt} = k_3[W]_T[R_2SO] \qquad (8)$$

Therefore, the change in $[R_2SO]$ should fit to a first-order exponential equation with $k_\psi = k_3[W]_T$. Indeed, the changes in the intensity of the sulfoxide signals with time (after the sulfide was completely disappeared, Fig. 1) fit very well to Eq. (2), and the values of the second-order rate constants (k_3) for the oxidation of sulfoxide by H_2O_2 catalyzed by **A** and **B** were calculated from the pseudo-first-order rate constant, $k_\psi = k_3[W]_T$. The rate constants, k_2 and k_3, for oxidation of different sulfides with H_2O_2 catalyzed by **A** and **B** and their ratios are summarized in Table 2.

3.5.1. Direct oxidation of the sulfoxide

In the above method, sulfoxides were generated as intermediates during the reaction, and are further oxidized to the corresponding sulfones. Therefore, the rate constants for the sulfoxide oxidation (k_3) were not determined independently, and are subject to error. To confirm the values of k_3, kinetic studies were carried out directly on the oxidation of methylphenylsulfoxide by H_2O_2 catalyzed by both catalysts (**A** and **B**). An NMR method was used under pseudo-first-order conditions. In the presence of large excess H_2O_2 over the catalyst and the sulfoxide (H_2O_2:cat:sulfoxide/5000:1:50), the reactions follow first-order kinetics, and therefore, Eq. (8) is applied with $k_\psi = k_3[W]_T$. The intensity–time curves were fit well to Eq. (2) (Fig. 6). The observed-first-order rate constants (k_ψ) varied linearly with the [catalyst] (Fig. 6 inset), and the second-order rate constants for the oxidation of methylphenolsuloxide were calculated from the slopes, $k_3 = k_\psi/[W]_T$. The values of k_3 (4.4 ± 0.2 and 2.8 ± 0.1 M^{-1} s^{-1} for **A** and **B**, respectively) obtained by this direct method agree with the k_3 values determined from the oxidation of thioanisol (Table 2).

In all cases, the rate constants for the oxidation of sulfoxides (k_3) by **A** are higher than the rate constants of the reactions catalyzed by **B**. However, an opposite trend was found in the case of the sulfide oxidation (k_2). Also, the ratios of k_2/k_3 for the reactions that are catalyzed by **B** is almost three times higher

than the corresponding ratios for the reactions catalyzed by **A**. The maximum amounts of sulfoxide ([sulfoxide]$_{max}$) formed in the catalyzed reactions with both catalysts and the time needed to reach this maximum (t_{max}) depend on the value of k_2/k_3, see Fig. 1. As the ratio of k_2/k_3 increases, the [sulfoxide]$_{max}$ increases and t_{max} (Eq. (9)) decreases [32]:

$$t_{max} = \frac{\ln(k_3/k_2)}{k_3 - k_2} \qquad (9)$$

The k_2/k_3 ratio also reflects the selectivity of the catalytic system to oxidize the sulfide to the sulfoxide over further oxidation of the sulfoxide, and the electrophilic versus nucleophilic nature of the active form of the catalyst. The lower activity of **B** toward sulfoxide oxidation confirms the effect of adding a nitro group on the electrophilicity of **B**, since sulfoxides are electrophilic reductants [30].

3.6. The proposed mechanism

The kinetic results obtained from studying the rate law agree with the general reaction mechanism shown in Scheme 2. The most important step is probably the oxygen-atom-transfer step
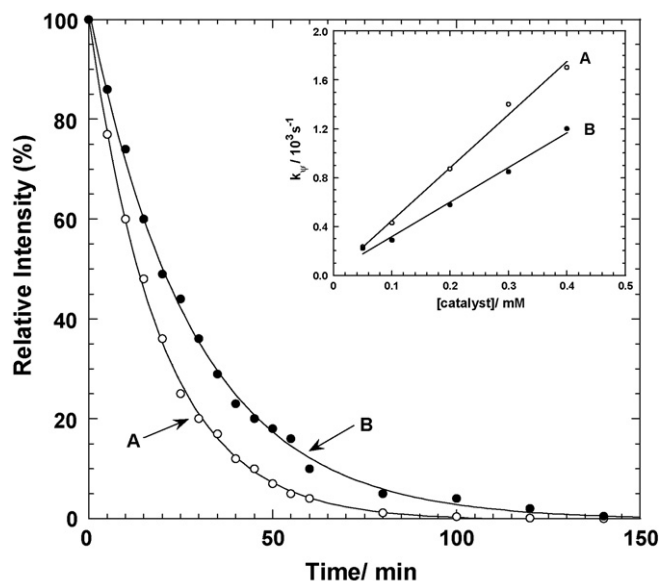

Fig. 6. The changes in the relative peak intensities with time of methylphenylsulfoxide (at $\delta = 2.73$ ppm) during the oxidation by H_2O_2 catalyzed by **A** (opened legend) and **B** (closed legend) in CD_3OD/D_2O (9/1) at 25 °C with $[H_2O_2] = 1.0$ M, [methylphenylsulfoxide] = 0.02 M and [cat] = 0.2 mM. The inset shows the variation of the observed-first-order rate constant (k_ψ) with the [catalyst].

(the oxidation step). Radical reaction has been ruled out because molecular oxygen had no effect on the rate of sulfide oxidation, and when acrylonitrile (a radical scavenger) is added to the reaction mixture no precipitate was formed. In addition, the negative values of the reaction constant ($\rho \sim -1.2$, Fig. 3) obtained by Hammett correlation indicates a build up of a positive charge upon the formation of the highest energy transition state during the reaction. Similar ρ values for the catalytic oxidation of sulfides by H_2O_2 have been reported previously [5a,31], and suggested the involvement of an oxygen-atom transfer as shown below:
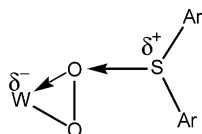
This may be occurred in a transition state or forms as a short-lived intermediate followed by a complete oxygen abstraction. An early study on the oxidation of organic sulfides by t-BuOOH catalyzed by $H_5PV_2Mo_{10}O_{40}$ has suggested a radical mechanism [33]. In contrast to the results obtained in this study, the rates of sulfide oxidation to sulfoxide do not correlate with the sulfide nucleophilicity or its redox potential. For example, the rate for oxidation of thioanisole was about six times slower than that for oxidation of diphenyl sulfide. Also, addition of water reduces the catalyst' activity, and the reaction rate was found to be inversely proportional to $[H_2O]$. In this study, however, when the ratio of water in the solvent mixture was increased from 1:9 to 1:1 ($H_2O:CH_3OH$) the reaction rate increased. This result rules out the possibility of binding the sulfide to the metal prior to the oxygen transfer. In such mechanisms, the reaction is usually inhibited by adding basic ligands including water [34]. It may suggest the formation of a polar transition state (or intermediate) relative to the reactants. The above transition state is more polar than the separate reactants, and it involves a charge separation. Furthermore, we found that the rate of oxidation of the sulfide by H_2O_2 catalyzed by B increases with the solution acidity. The dependence of the reaction rate on $[H^+]$ was linear in the range from 0.1 to 0.01 M. This is may be attributed to the protonation of the peroxo species (as shown below) which enhances its electrophilicity and polarizability. Therefore, the reactivity toward a soft-nucleophilic reductant, such as sulfide, is increased.
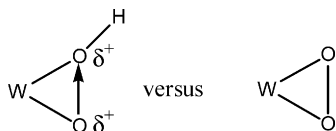
The activation parameters obtained from the variation of the catalyzed rate constants for the oxidation of thioanisol with temperature in the range 10–40 °C are listed below. The negative $\Delta S^{\ddagger}$ values usually point out to an associative transition state.

W-catalyst	$\Delta H^{\ddagger}$ (kJ/mol)	$\Delta S^{\ddagger}$ (J/mol)
A	64 ± 2	−34 ± 7
B	56 ± 4	−36 ± 10

Based on the reaction products and the kinetic results, the catalytic cycle for oxidation of sulfide by H_2O_2 cat-
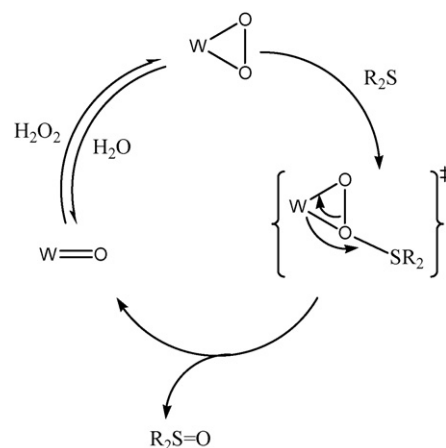
Scheme 3. The proposed mechanism.

alyzed by the polyperoxotungstate catalysts is proposed, Scheme 3.

In this mechanism, the oxygen-transfer from the active W-peroxo group to the sulfide is the rate-controlling step. This is most probably a concerted step that involves a transition state in which an external attack of the sulfide onto one of the peroxy-oxygen takes place. This is followed by heterolytic cleavage of the O–O bond (and the M–OO), and end up with a complete O-transfer to the sulfide yielding the sulfoxide and the W-oxo species. Then, the active species (W-peroxo) is regenerated from the reaction of the W-oxo species with H_2O_2.

4. Conclusion

The kinetic results of this study show clearly that the new catalyst (**B**) with a nitrophenyl group is more active toward sulfide oxidation by H_2O_2 than **A** which contains unsubstituted phenyl group, and **B** is less active toward sulfoxide oxidation under similar conditions. This modification is in the route for more rapid and selective formation of sulfoxides from sulfides. The kinetic findings also support the suggested mechanism shown in Scheme 3. The mechanism is limited to one active species, the peroxo form which is shown in Scheme 1. Previous studies have shown that the polyperoxometalates (with a maximum number of peroxo groups) are usually the most active and their formation from the parent polyoxometalates in the presence of excess H_2O_2 is rapid [15,35]. It is also possible that other species, with less number of peroxo groups, are active toward oxidation reactions. Kinetically, it would be very complicated to study all these peroxo species together. Therefore, most kinetic experiments were carried out with high H_2O_2 in which the catalyst exists with the maximum number of peroxo groups, and the involvement of other forms of the catalyst is negligible.

In order to explore the catalytic activity of the new catalyst toward other oxidations, kinetic studies on the oxidation of other organic substrates, such as olefins, by H_2O_2 catalyzed by these polyperoxotungstate catalysts (**A** and **B**) are conducted in our laboratory now, and the higher activity of **B** is also observed.

Acknowledgments

References

[1] (a) V. Nardello, J.M. Aubry, D.E. De Vos, R. Neumann, W. Adam, R. Zhang, J.E. ten Elshof, P.T. Witte, P.L. Alsters, J. Mol. Catal. A 251 (2006) 185;
(b) J. Hofmann, U. Freier, M. Wecks, A. Demund, Top. Catal. 33 (2005) 243;
(c) G. Grigoropoulou, J.H. Clark, J.A. Elings, Green Chem. 5 (2003) 1.
[2] (a) R. Noyori, M. Aoki, K. Sato, Chem. Commun. 16 (2003) 1977;
(b) G. Strukul (Ed.), Catalytic Oxidation with Hydrogen Peroxide as Oxidant, Kluwer Academic Publishers, London, 1992;
(c) B. Trost, Y. Masuyama, Teterhedron Lett. 25 (1984) 173.
[3] I.W.C.E. Arends, R.A. Sheldon, Top. Catal. 19 (2002) 133.
[4] L.F. Ramirez-Verduzco, E. Torres-Garcia, R. Gomez-Quintana, V. Gonzalez-Peña, F. Murrieta-Guevara, Catal. Today 98 (2004) 289.
[5] (a) F.E. Kuhn, A.M. Santos, W.A. Herrmann, J. Chem. Soc., Dalton Trans. (2005) 2483;
(b) F.E. Kuhn, A. Scherbaum, W.A. Herrmann, J. Organomet. Chem. 689 (2004) 4149;
(c) G. Soldaini, Synth. Lett. (2004) 1849;
(d) A.M. Ajlouni, J.H. Espenson, J. Am. Chem. Soc. 117 (1995) 9243;
(e) A.M. Ajlouni, J.H. Espenson, J. Org. Chem. 61 (1996) 3969.
[6] M. Ziolek, Catal. Today 90 (2004) 145.
[7] R.A. Sheldon, J. Dakka, Catal. Today 19 (1994) 215.
[8] R.A. Sheldon, I.W.C.E. Arends, H.E.B. Lempers, Catal. Today 41 (1998) 387.
[9] (a) C.L. Hill, J. Mol. Catal. A 262 (2007) 2;
(b) C.L. Hill, Chem. Rev. 98 (1998) 1;
(c) C.L. Hill, C.M. Prosser-McCartha, Coord. Chem. Rev. 143 (1995) 407.
[10] N. Mizuno, K. Yamaguchi, K. Kamata, Coord. Chem. Rev. 249 (2005) 1944.
[11] (a) N.M. Gresley, W.P. Griffith, A.C. Laemmel, H.I.S. Nogueira, B.C. Parkin, J. Mol. Catal. 117 (1997) 185;
(b) H.S. Schultz, H.B. Freyermuth, S.R. Buck, J. Org. Chem. 28 (1963) 1140.
[12] K. Sato, M. Hyodo, M. Aoki, X.-Q. Zheng, R. Noyori, Tetrahedron 57 (2001) 2469.
[13] S. Saaguchi, S. Watase, Y. Katayama, Y. Sakata, Y. Nishiyama, Y. Ishii, J. Org. Chem. 59 (1994) 5681.
[14] C. Venturello, R. Aloiso, J. Org. Chem. 53 (1988) 1553.
[15] W. Griffith, B. Parkin, A. White, D. Williams, J. Chem. Soc., Dalton Trans. (1995) 3131.
[16] K. Kaczorowska, Z. Kolarska, K. Mitka, P. Kowalski, Tetrahedron 61 (2005) 8315.
[17] N.S. Simpkins, in: N.S. Simpkins (Ed.), Sulfones in Organic Synthesis, Pergamon Press, Oxford, 1993.
[18] A.G. Renwick, L.A. De Damani, in: A.G. Renwick, L.A. De Damani (Eds.), Sulfur-Containing Drugs and Related Organic Compounds. Part B, vol. 1, Ellis Horwood, Chichester, UK, 1989, p. 133.
[19] H. Mei, B.W. Mei, T.F. Yen, Fuel 82 (2003) 405.
[20] F.M. Collins, A.R. Lucy, C. Sharp, J. Mol. Catal. A 117 (1997) 397.
[21] F. Figueras, J. Palomeque, S. Loridant, C. Fèche, N. Essayem, G. Gelbard, J. Catal. 226 (2004) 25.
[22] V. Hulea, F. Fajula, J. Bousquet, J. Catal. 198 (2001) 179.
[23] V. Hulea, P. Moreau, F. Di Renzo, J. Mol. Catal. A 111 (1996) 325.
[24] V. Hulea, P. Moreau, J. Mol. Catal. A 113 (1996) 499.
[25] R.S. Reddy, J.S. Reddy, R. Kumar, P. Kumar, J. Chem. Soc., Chem. Commun. (1992) 84.
[26] N.N. Trukhan, A.Yu. Derevyankin, A.N. Shmakov, E.A. Paukshtis, O.A. Kholdeeva, V.N. Romannikov, Micropor. Mesopor. Mater 44–45 (2001) 603.
[27] P.S. Raghavan, V. Ramaswamy, T.T. Upadhya, A. Sudalai, A.V. Ramaswamy, S.J. Sivasanker, J. Mol. Catal. A 122 (1997) 75.
[28] M.M. Lakouraj, M. Tajbakhsh, H. Tashakkorian, Lett. Org. Chem. 4 (2007) 75.
[29] E.I. Buneeva, S.V. Puchkov, O.N. Yarysh, A.L. Perkel, J. Anal. Chem. 53 (1998) 775.
[30] J.R.L. Smith, B.C. Gilbert, A.M. Payeras, J. Murray, T.R. Lowdon, J. Oakes, R.P. Prats, P.H. Walton, J. Mol. Catal. A 251 (2006) 114.
[31] K.A. Vassel, J.H. Espenson, J. Inorg. Chem. 33 (1994) 5491.
[32] J.H. Espenson, Chemical Kinetics and Reaction Mechanisms, 2nd ed., McGraw-Hill, New York, 1995, pp. 70–73.
[33] R.D. Gall, M. Faraj, C.L. Hill, Inorg. Chem. 33 (1994) 5015.
[34] P. Chaumette, H. Mimoun, L. Saussine, J. Fischer, A. Mitschler, J. Organomet. Chem. 250 (1983) 291.
[35] D.C. Duncan, R.C. Chambers, E. Hecht, C.L. Hill, J. Am. Chem. Soc. 117 (1995) 681.